Effect of induced electric field on single-file reverse osmosis

M. E. Suk and N. R. Aluru*

Received 19th February 2009, Accepted 2nd June 2009
First published as an Advance Article on the web 22nd July 2009
DOI: 10.1039/b903541a

We investigated the effect of the electric field on single-file reverse osmosis (RO) water flux using molecular dynamics simulations. The electric field is generated by introducing oppositely charged biomolecules to the salt solution and pure water chambers attached to the nanopore. Simulation results indicate that an electric field in the direction of RO enhances the water flux while in the direction opposite to RO it suppresses the water flux. When the RO water flux is enhanced, the single-file water dipoles are aligned in the direction of the electric field. The addition of an electric field in the direction of RO led to a flux of 3 water molecules ns^{-1} by constantly maintaining water dipole vectors in the direction of the electric field, and this water flux is superimposed on the pressure driven water flux.

I. Introduction

Water shortage is a global issue that is of utmost importance to both developing and developed nations.[1] A recent review by Shannon *et al*.[2] provides a good summary of the various issues, advances and challenges in the area of water purification. Clearly, advances in nanotechnology—including design of new membranes for fast desalination—can have a significant impact on water purification.

Reverse osmosis (RO) membranes are currently the most commonly used filtration membranes to remove ions and emerging pollutants. RO membranes can produce clean and potable water from seawater and saline aquifers occupying 97.5% of water on earth.[2] In an earlier study, we focused on energy efficient single-file reverse osmosis of water using carbon and boron nitride nanotubes.[3] The permeation coefficient of carbon nanotube (CNT) and boron nitride nanotube (BNNT) membranes was an order of magnitude higher compared to that of a polymethyl methacrylate (PMMA) membrane. Experiments and computational studies on CNT membranes revealed several orders of magnitude higher water fluxes compared to continuum hydrodynamics.[4–7]

In addition to the type of the membrane used, several other factors can affect water flux and controlling these can lead to efficient membrane separation technology. Raghunathan and Aluru showed that osmotic water flux through a negatively charged pore is higher compared to the osmotic water flux in a positively charged pore followed by the osmotic water flux in the uncharged pore.[8] They also showed that osmotic water flux depends on the size-asymmetric property of electrolytes due to a differential cation and anion affinity.[9] Gong *et al*.[10] showed that an asymmetric charge arrangement on the pore can pump water in one direction as fast as 4.4 water molecules ns^{-1} due to an asymmetric potential between the two ends of the pore. The effect of the electric field on fluids confined in the nanopore has been studied by Dzubiella *et al*.[11] They induced an electric field by imbalance of net charges of ions in the reservoirs. An induced electric field contributed to wetting of hydrophobic nanopore by coupled transport of water and ions. After ion permeations, the induced electric field vanishes, and the nanopore stops conducting water and ions, demonstrating voltage gating of the ion channel. Vaitheeswaran *et al*. studied the effect of the electric field on single-file water molecules confined in (6,6) nonpolar CNT using the Monte Carlo simulation.[12] They observed that the dipole orientation of single-file water molecules depends on the direction of the electric field.

Recently, it was shown that dipole orientation of water molecules confined in the nanoscale tube can induce a net water flux in the direction of the dipole vector without any external driving force, and this phenomenon was explained by rotation–translation coupling of water molecules.[13] In this paper, we investigate the effect of the electric field induced across an RO membrane on the dipole orientation of water molecules and on the RO water flux. Simulation results indicate that the water flux is higher when the dipole vector is in the direction of RO compared to the water flux when the dipole vector is in the opposite direction of RO.

II. Simulation methods

A schematic and a snap shot of the simulation set-up are shown in Fig. 1a and b, respectively. The system consists of a membrane with a nanopore, solution chamber, pure water chamber and pressure pistons. Single walled (6,6) BNNT is used as the nanopore. Lennard-Jones (LJ) parameters for boron and nitrogen atoms are taken from ref. 14. The diameter and length of the BNNT are 0.83 and 2 nm, respectively. The solution chamber contains water and 4M KCl. A simple point charge-extended (SPC/E) model was used for water and the ions were modeled as charged LJ atoms.[15] The pure water chamber contains only water molecules. The pressure pistons were made of silicon atoms with a GROMOS96 force-field. By applying external forces on pressure pistons, the z-location of

Department of Mechanical Science and Engineering, Beckman Institute for Advanced Science and Technology, University of Illinois at Urbana-Champaign, Urbana, IL 61801, USA.
E-mail: aluru@illinois.edu; Web: http://www.illinois.edu/~aluru/

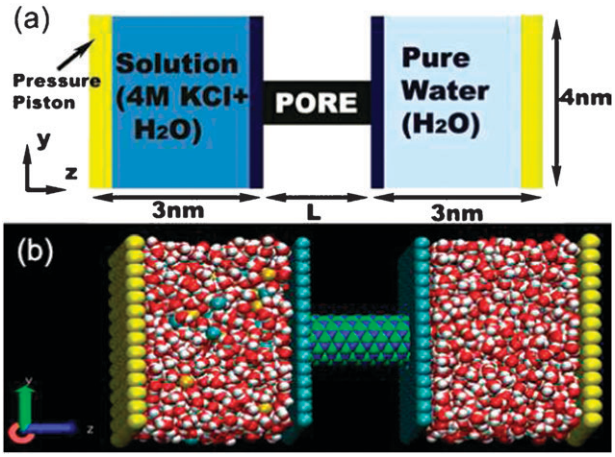

Fig. 1 (a) Schematic and (b) snapshot of the simulation set-up.

the pressure pistons is independently self-adjusted to maintain the desired pressure.[16] The z-component of the force, $f_z = (\sum_{i=1}^{M}\sum_{j=1}^{N} f_{zij} + AP_{ext})/M$, is applied on the pressure piston atoms. M and N are the number of molecules in the pressure piston and liquid, respectively, f_{zij} is the z component of the force acting on the ith pressure piston molecule due to the jth liquid molecule, A is the cross-sectional area of the chamber and P_{ext} is the external pressure. The first term is the average force between piston molecules and liquid molecules, applied in order to prevent the distortion of the pressure piston. The second term is the external force applied to maintain the desired pressure. Periodic boundary conditions are applied in the x- and y-direction. In the z-direction, a three-dimensional correction term introduced by Yeh and Berkowitz[17] and an enlarged box size (20 nm including vacuum) is used to remove the periodicity.[18,19]

Molecular dynamics (MD) simulations were performed using GROMACS 3.3.1.[20] A Nosé-Hoover thermostat with a time constant of 0.1 ps was employed to maintain the temperature of the fluid at 300 K. The electrostatic interaction was calculated using the particle mesh Ewald (PME) method[21] with a 0.1 nm real-space cutoff, 1.5 Å reciprocal space gridding, and splines of the order of 4 with a 10^{-5} tolerance.[21] A cutoff distance of 1 nm was used in calculating the LJ interaction. The SETTLE algorithm was used to constrain the geometry of water molecules. The equations of motion were integrated by using a leap-frog algorithm. The simulation time step was 1.0 fs and the trajectories were sampled every 1.0 ps for analysis. Each chamber was equilibrated for 2.0 ns by blocking the pore, and external pressure was applied for 1.0 ns before opening the pore to prevent initial osmosis. A pressure piston attached to the pure water chamber was maintained at 100 MPa, and different pressures ranging from 100 to 600 MPa were applied to the pressure piston attached to the solution chamber. After removing the pore blocks, the water molecules moved from the solution chamber to the pure water chamber against the osmotic pressure gradient while the ions did not go through. Simulation was run until at least 180 water molecules were transported to the pure water chamber.

To induce the electric field, we used lysine and aspartic acid carrying a positive charge and a negative charge at neutral pH, respectively. The LJ parameters and partial charges are taken from the updated Gromos96 force-field for improved hydration free enthalpy.[22] To induce the electric field in direction of RO ($+z$-direction), we put one lysine molecule in the solution chamber and one aspartic acid molecule in the pure water chamber. To induce an electric field in the direction opposite to RO ($-z$-direction), we put one lysine molecule in the pure water chamber and one aspartic acid molecule in the solution chamber. Since no ions permeate through the nanopore, the induced electric-field is maintained during the course of the simulation.

The electric-field screening effect of BNNT is negligible compared to CNT due to the wide band gap ($\sim$5.5 eV) of BNNT. Guo *et al.*[23] performed *ab initio* investigations of full static dielectric response of BNNT. Calculated axial permittivity of (6,6) BNNT based on the theory developed by Guo *et al.* is 6.5. Due to an electrostatic attraction, amino acids are found near the membrane wall. Thus, the estimates of induced field strength inside the pore can be calculated by assuming two charged slabs enclosing a medium with permittivity, ε_m and a pore with permittivity, ε_p.[24] The calculated electric field strength at the center of the pore is 1.1 V nm^{-1} assuming BNNT is non-polar ($\varepsilon_p = 1$) and screened electric-field strength due to pore permittivity of BNNT ($\varepsilon_p = 6.5$) is 1.03 V nm^{-1}. Since the screening effect of BNNT is small, we will assume that BNNT is non-polar in the calculations presented below.

III. Results and discussion

Simulations were performed without an induced electric field, and with a positive and negative induced electric field. The water flux for each ΔP case was calculated by dividing the total number of water molecules transported from the solution chamber to the pure water chamber by the total simulation time. Water flux varies linearly with the applied ΔP as expected from the irreversible thermodynamics model. As reported earlier, linear behavior does not necessarily require a small pressure gradient[25] due to an insignificant change in the water configuration inside the pore. We observed a higher water flux for RO with a positive electric field followed by the water flux with no electric field and with negative electric field (see Fig. 2). Comparing the water flux obtained with the positive electric field to that of the negative electric field, the water flux difference is almost constant regardless of the external pressure gradient. The water flux obtained without any electric field is in-between the two electric field cases.

The presence of an induced electric field controls the dipole orientation of water molecules confined in the nanopore. As shown in the inset snapshot of Fig. 3, the dipole vectors of all water molecules inside the (6,6) BNNT point in the same direction, either toward the solution reservoir or the pure water reservoir depending on the direction of the electric field. The water dipole vector is defined such that it points from the water oxygen to the center of mass of its hydrogen atoms. We averaged the angle between dipole vectors of water molecules inside the pore and the tube axis z at each sampling time, and

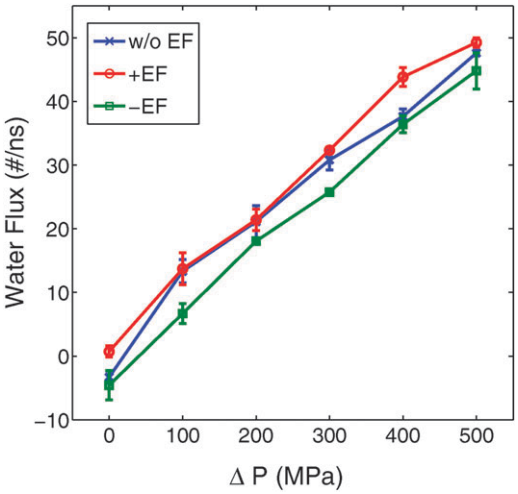

Fig. 2 Variation of the RO water flux with the applied pressure gradient for BNNT without an electric field (w/o EF), with a positive electric field (+EF) and with a negative electric field (−EF). Water flux with a positive electric field is higher compared to the water flux with a negative electric field. Water flux without an electric field is in-between the two electric field cases. A negative water flux implies that the flow is from the pure water chamber to the solution chamber, which is due to osmosis of water.

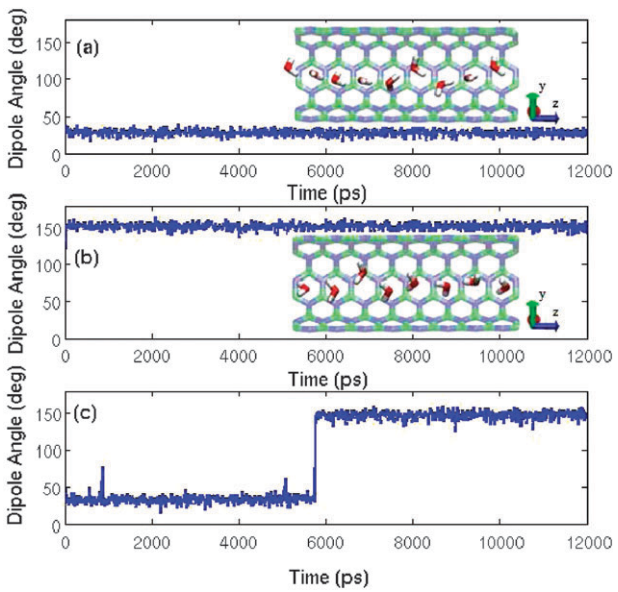

Fig. 3 Averaged water dipole angle with time when (a) positive electric field (b) negative electric field and (c) no electric field is induced. Applied pressure gradient is 300 MPa. The dipole angle is defined as the angle between water dipolevector and positive z axis. Dipole orientation angle is about 30° when a positive electric field is induced and the dipole vector points toward pure water reservoir. The dipole orientation angle is about 150° when a negative electric field is induced and the dipole vector points towards the solution reservoir

they are plotted in Fig. 3. Water dipole vector points towards the pure water reservoir for positive electric field (see Fig. 3(a)) and towards the solution reservoir for negative electric field (see Fig. 3(b)). In the absence of an electric field, dipole vectors of water molecules inside the (6,6) BNNT flip (see Fig. 3(c)).

Table 1 Dipole orientation time fraction ($P_{+\text{dipole}}$) for RO simulation with positive electric field (+EF), negative electric field (−EF) and no electric field (w/o EF)

ΔP/MPa	0	100	200	300	400	500
+EF	1	1	1	1	1	1
−EF	0	0	0	0	0	0
w/o EF	0.59	0.82	0.55	0.55	0.44	0.79

The dipole time fraction of dipole vector pointing towards the pure water reservoir can be calculated using $P_{+\text{dipole}} = T_{\theta<90}/T$ where $T_{\theta<90}$ is the total time when the dipole orientation angle, θ, is less than 90° and T is the total simulation time. Therefore, $P_{-\text{dipole}} = 1 - P_{+\text{dipole}}$. $P_{+\text{dipole}}$ for different pressure gradients is summarized in Table 1. For an equilibrium simulation with identical reservoirs connecting the pore, this value should be 0.5 if the simulation time is sufficiently long. For a reverse-osmosis simulation without an electric field, the preference of the dipole angle is not clear. To understand the effect of dipole orientation on water flux, we separated the two different dipole states of RO simulation without an electric field, and calculated the water flux corresponding to each dipole state (see Fig. 4). +dipole denotes the water flux when the dipole vector points towards the pure water reservoir and −dipole denotes the water flux when the dipole vector points towards the solution reservoir. Fig. 4 shows that the water flux for the +dipole state is always higher than that of the −dipole state. This indicates that a positive electric field, maintaining a +dipole state, gives the upper limit of water flux, while the negative electric field maintains the dipole vector pointing towards the solution reservoir, and gives the lower limit of water flux for a given pressure gradient.

To confirm the dependence of water flux on the dipole orientation, an equilibrium simulation was performed without

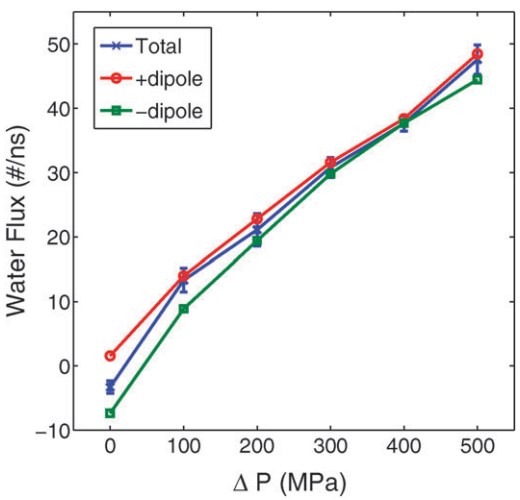

Fig. 4 Water flux corresponding to each dipole state for RO simulation without electric field. +dipole denotes the water flux when the dipole vector points towards the pure water reservoir and −dipole denotes the water flux when the dipole vector points towards the solution reservoir. Total water flux is the water flux calculated for the entire time. Water flux for +dipole state is higher than that for the −dipole state. Total water flux depends on the dipole time fraction

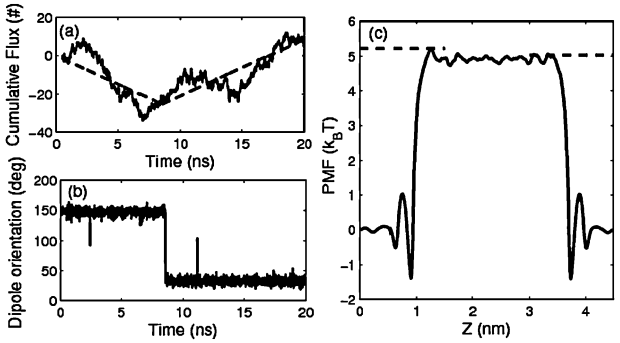

Fig. 5 (a) Cumulative flux and (b) dipole orientation as a function of time for equilibrium simulation. Cumulative flux is calculated by counting water molecules translocated through the pore. Water molecules are added if they translocate from left to right reservoir and subtracted if they translocate from right to left reservoir. Average water flux is −2.99 #/ns (dashed line from 500 ps to 8.52 ns) when dipole vector points towards the left reservoir and +2.96 #/ns (dashed line from 8.52 ns to 20 ns) when dipole vector points towards the right reservoir. (c) Potential of mean force profile of water molecules when dipole orientation of water molecules is greater than 90° (from 500 ps to 8.52 ns). Energy barrier at the pore entrance is slightly smaller in the right compared to the left.

an electric field, external pressure gradient and concentration gradient. Both reservoirs are filled with pure water, and simulation is run at 300 K using NVT ensemble for 20 ns. The cumulative water flux and the dipole orientation are plotted in Fig. 5a and b, respectively. Although there is fluctuation due to the high thermal velocity, water molecules are predominantly transported in the direction of dipole vector. From 0 to 8.52 ns, the water dipole vector pointed to the left reservoir and water flux was about −2.99 water molecules ns^{-1} (calculated after 500 ps filling and initialization time). From 8.52 to 20 ns, the water dipole vector pointed to the right reservoir, and water flux was about +2.96 water molecules ns^{-1}. The water flux difference between these two different states is 5.95 water molecules ns^{-1}, and it is close to the average water flux difference of 5.93 water molecules ns^{-1} between positive electric field and negative electric field in reverse osmosis simulation. The mechanism governing water translocation in the direction of the dipole vector has been explained recently by the rotation-translation coupling of water molecules confined in the nanopore.[13]

We also examined the equilibrium potential of mean force (PMF)[26] when the dipole vector pointed to the left reservoir from 500 ps to 8.52 ns (see Fig. 5c). It is known that there is a significant energy barrier at the pore entrance.[3,27] The energy barrier at the pore entrance interfacing left reservoir and right reservoir is 5.214 k_BT and 5.028 k_BT, respectively. They are measured at the first maxima from each end of the pore. This energy barrier difference (ΔE_b = −0.186 k_BT) also indicates the preferred translocation direction from the right reservoir to the left reservoir since the permeation is more favorable into the low-energy barrier. Such a unidirectional water transport due to the asymmetric potential has been studied elsewhere.[10] The potential of mean force can be decomposed by integrating the force components by other water molecules or membrane molecules.[28] The decomposition indicates that the energy barrier difference is caused by the water–water interaction supporting the possible mechanism of rotation–translation coupling of water molecules.[13]

Using Kramer's theory and linear approximation, the net flux, $J = k^+ - k^- = k_0(\Delta E_b/k_BT)$[29,30] where k^+ is forward hopping rate, k^- is backward hopping rate and k_0 is bidirectional hopping rate, $(k^+ + k^-)/2$. When the dipole orientation is not preserved, $k_0 = k^+ = k^-$, and k_0 is the equilibrium hopping rate.[31] Substituting ΔE_b (−0.186 k_BT) and k_0 (16.0 ns^{-1}),[3] the calculated net flux is −2.98 water molecules ns^{-1}, which is close to the observed net flux (−2.99 water molecules ns^{-1}). When the chemical potential gradient, $\Delta\mu$, is applied across the pore for reverse osmosis, the total energy barrier difference across the pore corresponds to $\Delta\mu + \Delta E_b$. Then, the net water flux is given by $J = k_0(\Delta\mu/k_BT) + k_0(\Delta E_b/k_BT)$. The first term is the water flux due to the chemical potential gradient and the second term is the water flux due to the single-file dipole orientation. This equation supports the superimposition of the water flux driven by the chemical potential gradient, which is due to the pressure gradient and the concentration gradient, and water flux due to the single-file dipole orientation as a result of induced electric field.

We can also introduce an additional equilibrium constant, $c = k_0(\Delta E_b/k_BT)$. Considering the dipole time fraction, $P_{+\text{dipole}}$ as defined above, generalized net water flux is given by

$$J = k_0(\Delta\mu/k_BT) + c(2P_{+\text{dipole}} - 1) \quad (1)$$

where c = 2.98 ns^{-1} and k_0 = 16 ns^{-1}. When there is no preference on the dipole orientation, $P_{+\text{dipole}}$ = 0.5 and $J = k_0(\Delta\mu/k_BT)$ as reported in other studies.[3,25,29,30] The water flux obtained by MD simulation and eqn (1) is compared in Fig. 6. $P_{+\text{dipole}}$ used in the calculation is specified in Table 1. Assuming an ideal solution and unity activity coefficient, the chemical potential gradient is calculated by integrating,

$$d\mu = k_BT \ln x + vdP/N_A \quad (2)$$

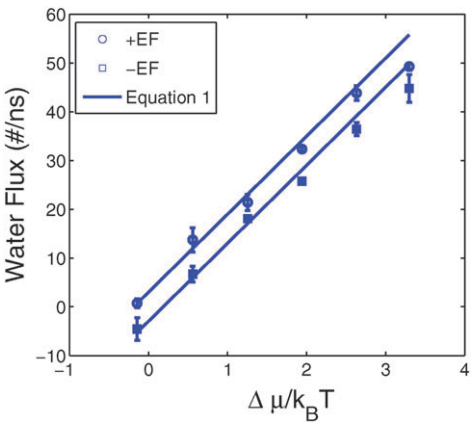

Fig. 6 Comparison of water flux obtained from the MD simulation (+EF and −EF) with that predicted from eqn (1). +EF and −EF denote RO water flux with positive electric field and negative electric field, respectively. The upper and lower solid line is calculated with $P_{+\text{dipole}}$ = 1 and $P_{+\text{dipole}}$ = 0, respectively.

where x is the molar concentration of water, v is the molar volume, P is the pressure, and N_A is the Avogadro number. The water fluxes from the RO simulation with positive electric field and negative electric field are in reasonable agreement with eqn (1) with $P_{+\text{dipole}} = 1$ and $P_{+\text{dipole}} = 0$, respectively. The reason for the deviation at high pressure can be due to the assumption of ideal solution in calculating the chemical potential.

Won *et al.*[32,33] showed that partial charges of (6,6) BNNT with a length of about 1.4 nm flipped the dipole orientation of water at the center of the pore, which resulted in the formation of L-defect at the center of the pore. We introduced the partial charges to investigate its effect on the RO water flux. We tested the BNNT saturated at the ends with hydrogen atoms to use the partial charges reported by Won *et al.*[32] Induced electric field still maintained the dipole vector of water molecules in the direction of the electric field, and we observed insignificant change of water flux when partial charges are introduced. With 300 MPa of pressure gradient and electric field induced in the positive z-direction, the water flux without partial charges and with partial charges was 37.7 water molecules ns^{-1} and 37.9 water molecules ns^{-1}, respectively. When the electric field is induced in the negative z-direction, the water flux without partial charges and with partial charges was 32.3 water molecules ns^{-1} and 34.3 water molecules ns^{-1}, respectively. The water flux through hydrogen terminated BNNT was about 6 water molecules ns^{-1} higher compared to that through naked BNNT due to the hydrophilicity at the pore entrance.[3,34]

In a prior study on reverse osmosis, it was observed that with ions as solutes the reverse osmosis flux through model membranes made of spherical LJ atoms and thin zeolite membranes was enhanced when periodically reversed electric field was applied.[35–38] When a static electric field was applied, reverse osmosis flux did not increase as ions permeated through the pore and clogged the pore. In addition, molecular orientation effects on reverse osmosis flux were not observed.[37] However, the results in this paper indicate that in the case of single-file water molecules confined inside a nanotube, molecular orientation can play an important role and have a significant effect on reverse osmosis.

IV. Conclusion

We investigated the effect of induced electric field by biomolecules on reverse osmosis. It was found that electric field induced in the direction of RO enhanced RO water flux and in the direction opposite of RO suppressed it. This result was explained based on the dipole orientation of water molecules confined in (6,6) BNNT. Water molecules in (6,6) BNNT formed single-file and their concerted dipole vectors pointed either toward the positive or negative axial direction of BNNT. In equilibrium MD simulation, we also observed net motion of single-file water molecules in the direction of dipole vectors. Consequently, induced electric field constantly maintained the dipole vector in the direction of electric field, and around 3 water molecules ns^{-1} of water flux driven by dipole vector was superimposed on the pressure driven water flux of RO. Without an external pressure gradient, the induced electric field in the direction of RO generated about 0.73 water molecules ns^{-1} of water flux against the osmotic potential corresponding to 4 M concentration gradient. For 1.12 M salt concentration of sea water, RO water flux close to about 2.7 water molecules ns^{-1} can be achieved without external pressure gradient. In summary, induced electric field can enhance RO water flux and can be used for energy efficient RO process.

Acknowledgements

This research was supported by NSF under Grants 0120978 (the Water CAMPWS Center), 0328162 (the nano-CEMMS Center), 0523435, and 0810294, and by NIH under Grant No. PHS 2 PN2 EY016570B.

References

1 T. Hillie and M. Hloph, *Nat. Nanotechnol.*, 2007, **2**, 663.
2 M. A. Shannon, P. W. Bohn, M. Elimelech, J. G. Georgiadis, B. J. Marinas and A. M. Mayes, *Nature*, 2008, **452**, 301.
3 M. E. Suk, A. Raghunathan and N. R. Aluru, *Appl. Phys. Lett.*, 2008, **92**, 133120.
4 J. K. Holt, H. G. Park, Y. Wang, M. Stadermann, A. B. Artyukhin, C. P. Grigoropoulos, A. Noy and O. Bakajin, *Science*, 2006, **312**, 1034.
5 M. Majumder, N. Chopra, R. Andrews and B. J. Hinds, *Nature*, 2005, **438**, 44.
6 S. Joseph and N. Aluru, *Nano Lett.*, 2008, **8**, 452.
7 G. Hummer, J. G. Rasaiah and J. P. Noworyta, *Nature*, 2001, **414**, 188.
8 A. V. Raghunathan and N. R. Aluru, *Phys. Rev. Lett.*, 2006, **97**, 024501.
9 A. V. Raghunathan and N. R. Aluru, *Appl. Phys. Lett.*, 2006, **89**, 064107.
10 X. Gong, J. Li, H. Lu, R. Wan, J. Li, J. Hu and H. Fang, *Nat. Nanotechnol.*, 2007, **2**, 709.
11 J. Dzubiella, R. J. Allen and J. P. Hansen, *J. Chem. Phys.*, 2004, **120**, 5001.
12 S. Vaitheeswaran, J. C. Rasaiah and G. Hummer, *J. Chem. Phys.*, 2004, **121**, 7955.
13 S. Joseph and N. Aluru, *Phys. Rev. Lett.*, 2008, **101**, 064502.
14 J. W. Kang and H. J. Hwang, *J. Phys.: Condens. Matter*, 2004, **16**, 3901.
15 S. Koneshan, J. C. Rasaiah, R. M. Lynden-Bell and S. H. Lee, *J. Phys. Chem. B*, 1998, **102**, 4193.
16 C. Huang, K. Nandakumar, P. Y. K. Choi and L. W. Kostiuk, *J. Chem. Phys.*, 2006, **124**, 234701.
17 I. C. Yeh and M. L. Berkowitz, *J. Chem. Phys.*, 1999, **111**, 3155.
18 A. Brodka and A. Grzybowski, *J. Chem. Phys.*, 2002, **117**, 8208.
19 D. Bostick and M. L. Berkowitz, *Biophys. J.*, 2003, **85**, 97.
20 E. Lindahl, B. Hess and D. van der Spoel, *J. Mol. Model.*, 2001, **7**, 306.
21 T. Darden, D. York and L. Pedersen, *J. Chem. Phys.*, 1993, **98**, 10089.
22 C. Oostenbrink, A. Villa, A. E. Mark and W. F. V. Gunsteren, *J. Comput. Chem.*, 2004, **25**, 1656.
23 G. Y. Guo, S. Ishibashi, T. Tamura and K. Terakura, *Phys. Rev. B*, 2007, **75**, 245403.
24 J. Dzubiella and J. P. Hansen, *J. Chem. Phys.*, 2005, **122**, 234706.
25 F. Zhu, E. Tajkhorshid and K. Schulten, *Phys. Rev. Lett.*, 2004, **93**, 224501.
26 R. Kjellander and H. Greberg, *J. Electroanal. Chem.*, 1998, **450**, 233.
27 C. Y. Won, S. Joseph and N. R. Aluru, *J. Chem. Phys.*, 2006, **125**, 114701.
28 B. Roux and M. Karplus, *Biophys. J.*, 1991, **59**, 961.

29 B. L. de Groot and H. Grubmuller, *Curr. Opin. Struct. Biol.*, 2005, **15**, 176.
30 B. L. de Groot, D. P. Tieleman, P. Pohl and H. Grubmüller, *Biophys. J.*, 2002, **82**, 2934.
31 A. Berezhkovskii and G. Hummer, *Phys. Rev. Lett.*, 2002, **89**, 064503.
32 C. Y. Won and N. R. Aluru, *J. Phys. Chem. C*, 2008, **112**, 1812.
33 C. Y. Won and N. R. Aluru, *J. Am. Chem. Soc.*, 2007, **129**, 2748.
34 J. Zheng, E. M. Lennon, H. Tsao, Y. Sheng and S. Jiang, *J. Chem. Phys.*, 2005, **122**, 214702.
35 S. Murad, R. Madhusudan and J. G. Powles, *Mol. Phys.*, 1997, **90**, 671.
36 S. Murad, K. Oder and J. Lin, *Mol. Phys.*, 1998, **95**, 401.
37 R. Madhusudan, J. Lin and S. Murad, *Fluid Phase Equilib.*, 1998, **150**, 97.
38 H. Yan, S. Murad and E. Enciso, *Fluid Phase Equilib.*, 2001, **183**, 279.